



UNIVERSITÀ
DEGLI STUDI
FIRENZE

FLORE

Repository istituzionale dell'Università degli Studi
di Firenze

**Dielectric Relaxation Spectroscopy of Lysozyme Aqueous Solutions:
Analysis of the delta-Dispersion and the Contribution of the**

Questa è la Versione finale referata (Post print/Accepted manuscript) della seguente pubblicazione:

Original Citation:

Dielectric Relaxation Spectroscopy of Lysozyme Aqueous Solutions: Analysis of the delta-Dispersion and the Contribution of the Hydration Water / C; Cametti; S. Marchetti; C.M.C. Gambi; G. Onori. - In: JOURNAL OF PHYSICAL CHEMISTRY. B, CONDENSED MATTER, MATERIALS, SURFACES, INTERFACES & BIOPHYSICAL. - ISSN 1520-6106. - STAMPA. - 115:(2011), pp. 7144-7152. [10.1021/jp2019389]

Availability:

This version is available at: 2158/529656 since:

Published version:

DOI: 10.1021/jp2019389

Terms of use:

Open Access

La pubblicazione è resa disponibile sotto le norme e i termini della licenza di deposito, secondo quanto stabilito dalla Policy per l'accesso aperto dell'Università degli Studi di Firenze (<https://www.sba.unifi.it/upload/policy-oa-2016-1.pdf>)

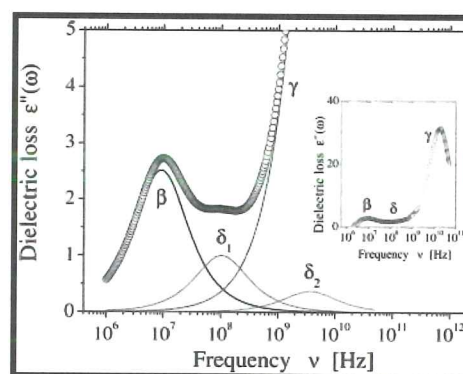
Publisher copyright claim:

(Article begins on next page)

Dielectric Relaxation Spectroscopy of Lysozyme Aqueous Solutions: Analysis of the δ -Dispersion and the Contribution of the Hydration Water

C. Cametti,^{†,*} S. Marchetti,[‡] C.M.C. Gambi,[‡] and G. Onori[§][†]Department of Physics and INFM CRS-SOFT, "La Sapienza" University of Rome, Piazzale A. Moro 5, I-00185, Rome, Italy[‡]Department of Physics, University of Florence and CNISM, Via G. Sansone 1, 50019 Sesto Fiorentino, Florence, Italy[§]Department of Physics and INFM CRS-SOFT, University of Perugia, Via G. Pascoli, Perugia, Italy

ABSTRACT: The dielectric properties of lysozyme aqueous solutions have been investigated over a wide frequency range, from 1 MHz to 50 GHz, where different polarization mechanisms, at a molecular level, manifest. The dielectric relaxation spectra show a multimodal structure, reflecting the complexity of the protein–water interactions, made even more intricate with the increase of the protein concentration. The deconvolution of the spectra into their different components is not unambiguous and is generally a delicate process which requires caution. We have analyzed the whole relaxation region, on the basis of the sum of simple Debye-type relaxation functions, considering three main contributions. Particular attention has been paid to the δ -dispersion, intermediate between the β -dispersion (rotational dynamics of the protein) and the γ -dispersion (orientational polarization of the water molecules). This intermediate contribution to the dielectric spectrum is attributed to the orientational polarization of water molecules in the immediate vicinity of the protein surface (hydration water). Our measurements clearly demonstrate that, at least at high protein concentrations, the δ -dispersion has a bimodal structure associated with two kinds of hydration water, i.e., tightly bound and loosely bound hydration water. In the concentration range investigated, the existence of a three-modal δ -dispersion, as recently suggested, is not supported, on the basis of statistical tests, by the analysis of the dielectric relaxations we have performed and a bimodal dispersion is accurate enough to describe the experimental data. The amount of the hydration water has been evaluated both from the dielectric parameters associated with the δ -dispersion and from the decrement of the loss peak of the γ -dispersion. The relative weight of tightly bound and loosely bound hydration water is briefly discussed.



1. INTRODUCTION

Water in the immediate vicinity of biomolecules, which is generally referred to as the hydration water, plays a crucial role in different aspects of biological processes.¹ There are many experimental techniques that allow, in principle, the investigation of dynamics and structure of hydration water on a protein surface, including calorimetry,² X-ray crystallography,³ neutron scattering,⁴ nuclear magnetic resonance,⁵ time-resolved fluorescence, and infrared spectroscopy.⁶ Among them, dielectric spectroscopy has the advantage to investigate arrangement of water in confined systems, more generally in interfacial or restricted environments, over a wide time scale, providing information on the orientational dynamics of molecular dipoles and covering all kinds of polarization fluctuations in the milli- to picosecond time scales.

Dielectric relaxation spectra of aqueous protein solutions generally extend over a broad frequency range, let us say from a few kHz to tens of GHz, consisting of different, and partially overlapping, regions, originated by different polarization mechanisms, at a molecular level. If on the one hand dielectric spectroscopy is a unique valuable technique in the investigation

of aqueous solutions, on the other hand, the presence of rather complex spectra does not always make easy and unambiguous their assignment to well-defined polarization mechanisms and the interpretation of the results requires caution.

As far as the protein solutions are concerned, several relaxation processes were observed and attributed to molecular mechanisms that involve motion of side groups in the protein conformation and of various layers of strongly and/or weakly bound water. In order of increasing relaxation frequency, the picture that has found a general consensus, strengthened by a large spread of investigations over the last decades, considers three main relaxation regions, named β , δ , and γ dispersions.^{7,8} They are unambiguously associated to the motion of the macromolecule as a whole (orientational relaxation of the protein dipole), to hydration water in the interfacial region surrounding the biomolecule (dipoles of the water molecules in the hydration shell) and, finally, to the orientational polarization of the water molecules

Received: February 28, 2011

Revised: April 8, 2011

Published: May 10, 2011

(bulk water dipoles), respectively.⁷ This scenario is made even more complicated by the presence of two further relaxation regions, due to the electrode polarization effect (falling in the low-frequency tail of the spectrum) and, in the presence of charged proteins, to the double layer ionic polarization. The former can be considered as an artifact, being, to a large extent, independent of the presence of the protein phase. It depends on the accumulation of simple ions in the proximity of the metal electrodes which cause the rising up of an ionic, frequency dependent, polarization which follows a scaling behavior $\sim A\omega^a$. The latter, i.e., the double layer ionic polarization, is originated by the apparent dipole moment due to an asymmetric ionic distribution of the ionic atmosphere at the protein surface, induced by the external electric field. This ionic polarization originates the so-called α -dispersion. Since the ionic electrode polarization effect produces a very large dielectric response, especially for highly conducting solutions, it may be difficult to resolve and characterize this region of the spectrum.

At a higher level of sophistication, the δ -dispersion, attributed to the hydration water, presents a composite structure, resulting in two (or even three) different overlapping relaxation regions. Recently, Oleinikova et al.⁹ have discussed in details the structure of the δ -dispersion and, from their analysis, they suggested the presence of three dispersion regions, numbered from low to high frequency by δ_1 , δ_2 , and δ_3 dispersions. The analysis of their data, based on Ribonuclease A in aqueous solution, assigns the δ_3 dispersion (≈ 5 GHz) to hydration water orientational polarization, the δ_2 dispersion (≈ 300 MHz) to polar side chain fluctuation and, finally, the δ_1 dispersion (≈ 10 MHz) to protein water cross correlation, this latter assignment being supported by MD simulation. However, the δ -dispersion was often considered bimodal^{10,11} and an alternative scenario attributes the bimodal nature of the δ -dispersion to two kinds of hydration water, i.e., *loosely* bound water (at 3–5 GHz) and *tightly* bound water (at 100 MHz). The first hydration layer, that interacts with the solvent-exposed protein atoms, consists of water molecules strongly bound to the roughness of the protein surface. A second layer, that is not in direct contact with the protein surface, consists of more loosely bound molecules which exchange with the tightly bound water, with properties approaching those of bulk water. Finally, a third component consists of surrounding water unaffected by the presence of proteins.

The attribution of the δ -dispersion, being of small dielectric strength, is a difficult task anyway, depending, at least in part, on the deconvolution technique adopted in order to isolate this contribution from the whole dielectric spectrum, since data processing can easily induce systematic errors.

In this work, we report on the dielectric spectra of an aqueous lysozyme solution in a wide concentration range, up to 125 mg/mL, over the frequency range from 1 MHz to 50 GHz, in order to cover the complete frequency extension of the three, β , δ , and γ , dispersions.

Lysozyme is one of the earliest characterized and most studied globular proteins. It is spheroidal in shape with highly compact conformation and is frequently used in studies of protein hydration.^{12,13} Despite the effects on protein–water interactions being studied repeatedly, no fully accepted picture emerges on hydrodynamic interactions and protein hydration. The above-stated features of lysozyme greatly simplify the interpretation of the dielectric spectra and this protein can be considered a model system which may contribute to clarify, in a well-controlled condition, the structure of the dielectric spectrum in its intermediate region, corresponding to the δ -region.

We preliminarily observed on the basis of a statistical F test that the dielectric spectra need to be analyzed by a different parametrization, depending on the lysozyme concentration. In particular, in the low concentration range, a monomodal δ -dispersion accounts for the experimental data with enough accuracy, whereas, in the high-concentration range, a bimodal δ -dispersion must be necessarily introduced.

The work is organized as follows. In Section II, we discuss in detail the analysis of the dielectric spectra and the cautions necessary in their deconvolution. In Section III, we assign the observed relaxation regions to different polarization mechanisms and, from each observed relaxation, we extract the relevant microscopic parameters associated to the protein. In this context, the structure of the δ -dispersion is discussed in depth. A comparison of our results with literature data is also reported. A brief conclusion is drawn in Section IV.

2. EXPERIMENTAL SECTION

2.1. Materials. Chicken egg-white lysozyme was obtained from Sigma (St. Louis, MS) and used without further purification. Samples (L-6876, CAS[12650–88–3]) contained lysozyme crystallized three times, dialyzed, and supplied as lyophilized powder, 95% protein by weight with the remainder sodium acetate and sodium chloride. The specific activity was 50 000 units/mg. From crystallographic structure, lysozyme can be described as an ellipsoid of semiaxes 13 and 22 Å, respectively (axial ratio 1.7). The molecular weight is 14.7 kDa and the partial specific volume is 0.73 mL/mg. The solutions were prepared by weighing and dissolving the protein in deionized water (electrical conductivity less than 10^{-6} mho/cm at room temperature). The protein concentration was varied in a relatively extended concentration range from 1 to 125 mg/mL. No buffer was used, so that the pH of the solution at an intermediate concentration ($C = 45$ mg/mL) had a value of about pH = 5.5. The protein is in its native state and bears, in these conditions, a positive net charge of about 10 elementary charges.¹⁴

In order to ascertain the possible presence of protein aggregates and to gain insight on the contribution of impurities present in the samples investigated, we measured the electrical conductivity of the protein solutions. The d.c. electrical conductivity σ_0 of the aqueous protein solutions as a function of the protein concentration, C , measured at the frequency of 1 kHz, is shown in Figure 1. The linear dependence of the electrical conductivity on the protein concentration rules out that protein aggregation might occur, at least in the concentration range investigated. Moreover, the dependence of the electrical conductivity on the temperature (a typical behavior for the concentration $C = 45$ mg/mL is shown in the inset of Figure 1) reproduces the one of a NaCl electrolyte solution with a molarity corresponding to the value expected on the basis of the sample composition. This finding ensures that the major part of the residues and impurity derives from a concentration of sodium chloride less than 5% of the protein weight.

2.2. Dielectric Measurements. The dielectric properties of the protein solutions were measured in the frequency range from 1 MHz to 50 GHz, by means of two different experimental setups. In the frequency range from 1 MHz to 2 GHz, we employed a computer-controlled Impedance Analyzer Hewlett-Packard mod. 4291A coupled with a dielectric cell consisting in a short section of a cylindrical coaxial cable excited far below its cut-off frequency. The cell was calibrated with liquids of known permittivity

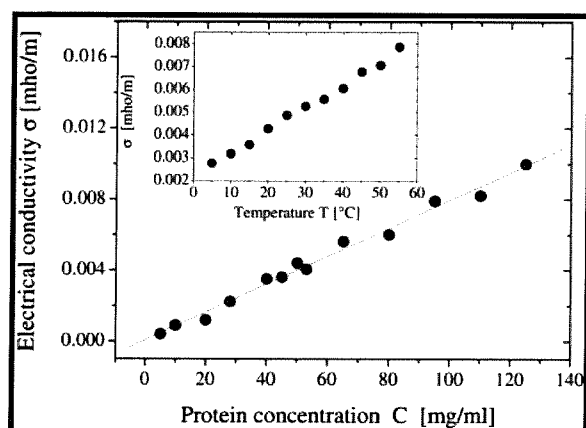


Figure 1. Electrical conductivity σ of aqueous lysozyme solution as a function of the protein concentration, C , at the temperature of 20 °C. The inset shown the electrical conductivity σ of aqueous lysozyme solution at the concentration $C = 45$ mg/mL, as a function of the temperature T .

and electrical conductivity according to a procedure previously reported.^{15,16}

In the frequency range from 500 MHz to 50 GHz, measurements were carried out by means of an Agilent N5230 Vector Network Analyzer (VNA), together with a dielectric kit probe Agilent 85070E. The probe is immersed in a protein solution under investigation, contained in a glass vessel. The solution is the electrical termination of the probe, that is a section of a transmission line.

The analyzers, in both of the two frequency ranges investigated, measure the complex reflection coefficient $\Gamma^*(\omega)$, from which the complex dielectric constant $\varepsilon^*(\omega)$ is obtained following the procedure reported by Bao et al.,¹⁷ through the relationship:

$$\varepsilon^*(\omega) = \frac{A_1^*(\omega)\Gamma^*(\omega) - A_2^*(\omega)}{A_3^*(\omega) - \Gamma^*(\omega)} \quad (1)$$

where $A_j(\omega)$ ($j = 1, 2, 3$) are frequency-dependent complex constants which can be obtained from calibration procedure performed with air, short connection, and Millipore water. All of the measurements have been carried out at 20 °C, controlled within 0.1 °C.

2.3. Analysis of the Dielectric Spectra. The dielectric and conductometric properties of aqueous lysozyme solutions present a rather complex behavior, showing dielectric spectra that clearly derive from different and, partially overlapping, polarization mechanisms. The a priori decision to establish how many different mechanisms, and consequently how many independent dielectric relaxations, are present is a difficult task and the procedure employed in the deconvolution of the spectra, no matter which they are, requires caution. Only in a second stage, a statistical test can offer some kind of support. Usually, one starts the analysis with a simple Debye function and carefully increases the number of relaxation processes and the free fitting parameters, simultaneously considering the use of more complex functions, such as Cole–Cole or Cole–Davidson relaxation functions.

Whereas the presence of the β - and γ -dispersion are well established, the problem arises in establishing how many sub-dispersions are present in the frequency interval where the so-called δ -dispersion falls. Following the hypothesis of maximum simplicity, we decided to analyze the δ -dispersion as due to a

single relaxation mechanism (in the low protein concentration range) and as due to double relaxation mechanisms (in the high protein concentration range). Accordingly, the above stated hypothesis, the whole relaxation function, modeled according to simple Debye-type relaxations, reads as follows:

$$\varepsilon^*(\omega) = \varepsilon_\infty + \frac{\Delta\varepsilon_\beta}{1 + i\omega\tau_\beta} + \frac{\Delta\varepsilon_\delta}{1 + i\omega\tau_\delta} + \frac{\Delta\varepsilon_\gamma}{1 + i\omega\tau_\gamma} + \frac{\sigma_0}{i\omega\varepsilon_0} \quad (2)$$

in the low lysozyme concentration (roughly up to 50 mg/mL) and,

$$\varepsilon^*(\omega) = \varepsilon_\infty + \frac{\Delta\varepsilon_\beta}{1 + i\omega\tau_\beta} + \frac{\Delta\varepsilon_{\delta_1}}{1 + i\omega\tau_{\delta_1}} + \frac{\Delta\varepsilon_{\delta_2}}{1 + i\omega\tau_{\delta_2}} + \frac{\Delta\varepsilon_\gamma}{1 + i\omega\tau_\gamma} + \frac{\sigma_0}{i\omega\varepsilon_0} \quad (3)$$

in the high lysozyme concentration (from 50 to 125 mg/mL). Here, $\Delta\varepsilon_j$ and τ_j ($j = \beta, \delta$, and γ) are the dielectric increment and the relaxation time of the various relaxation processes considered, ε_∞ the high-frequency limit of the permittivity and σ_0 the d.c. electrical conductivity. Finally, ε_0 is the permittivity of free space and ω the angular frequency of the applied electric field.

We are aware that this choice is a little bit arbitrary and that other possibilities could be certainly investigated. In particular, we point out that the Debye relaxation functions might be replaced more generally by Cole–Cole relaxation functions, with the introduction however of three further (in the first case, eq 2) and four further (in the second case, eq 3) parameters.

However, in the analysis of these data, where two different models involving a different number of parameters are applied, it is important to find a statistical test to decide whether a model is significantly better than the other to describe the same set of m observations. To decide this, the error sum S for each model (here denoted as S_A and S_B),

$$S = \sum_1^m W_i (X_i^{\text{obs}} - X_i^{\text{calcd}})^2 \quad (4)$$

can be used to calculate the function,

$$f(m, p, q) = \frac{(S_A - S_B)(m - p)}{S_B(q - p)} \quad (5)$$

where p and q are the number of free parameters of models A and B, respectively, which is assumed to be distributed according the F statistical function $F(q - p, m - q, \alpha)$, with $(q - p)$ and $(m - p)$ degrees of freedom. The weights have been assumed to be proportional to the inverse of the squares of the single experimental values. The values of F at $\alpha = 95\%$ confidence level, obtained in the two above data analyses, in spite of the scattering of the experimental values, attest that the relaxation function, eq 2, allows a “better” description of the experimental results than the one obtained on the basis of the relaxation function, eq 3, in the low-concentration range, let us say up to 45–50 mg/mL. In the higher concentration range, the opposite is true, and relaxation function eq 3 furnishes a better description of the data.

Considering this statistical approach, we analyzed the dielectric spectra on the basis of a dielectric model consisting of three dielectric dispersions (β , δ and γ -dispersions, respectively) in the low-concentration range, up to 45–50 mg/mL and consisting in four dielectric dispersions (β , δ_1 , δ_2 and γ -dispersions,

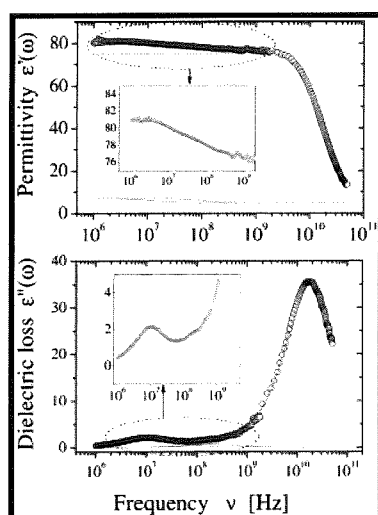


Figure 2. Dielectric spectra of lysozyme aqueous solution ($C = 28$ mg/mL) as a function of frequency at the temperature of 20 °C. Upper panel: the permittivity $\epsilon'(\omega)$ in the frequency range from 1 MHz to 50 GHz. The full lines represent the calculated values on the basis of eq 2. The inset shows in an enlarged scale the low-frequency tail of the spectrum and its deconvolution by two single Debye-type relaxation functions. Bottom panel: the dielectric loss in the same frequency range. The inset shows the deconvolution of the spectrum in its low-frequency tail.

respectively), in the high-concentration range, from 50 to 125 mg/mL. This choice is certainly not the unique possible choice, but it satisfies the requirement of the minimum number of parameters needed to obtain a meaningful (and consistent) description of the data, over the whole concentration range investigated.

Before proceeding any further, we want to comment a little bit more deeply the reliability of the data we present. The whole spectrum is acquired from two different experimental set ups, working in two different, but partially overlapping, frequency ranges. We obtained a very satisfactory agreement for the permittivity $\epsilon'(\omega)$ over the frequency range common to the two instruments, in spite of the fact that necessarily two different calibration procedures should be employed. As far as the dielectric loss $\epsilon''(\omega)$ is concerned, this quantity is derived from the total dielectric loss by subtracting the purely conductivity contribution, i.e., by subtraction the quantity $\sigma_0/(\epsilon_0\omega)$. This means that an independent measurement of the d.c. conductivity is required. We have measured the d.c. conductivity of the samples investigated at the frequency of 1 kHz and this value has been used for the extraction of the dielectric loss from the total dielectric loss also in the higher frequency range. The agreement is quite good. However, since the overlapping region falls around the frequencies between 500 MHz and 1 GHz, where there is the occurrence of the δ -dispersion, an incorrect combination of the data deriving from the two different instruments might cause a distortion of the spectrum, with the appearance (or the disappearance) of more than one contribution in the δ region. Moreover, we have accurately checked that, even if the d.c. conductivity σ_0 should be changed, at least within reasonable limits, this effect does not imply the need to vary the number of the conjectured dispersions. Moreover, the permittivity $\epsilon'(\omega)$ and the dielectric loss $\epsilon''(\omega)$, obtained from the total electrical conductivity $\sigma(\omega)$, satisfy the Kramer–Krönig relationship,¹⁸ ensuring the correctness of the procedure employed.

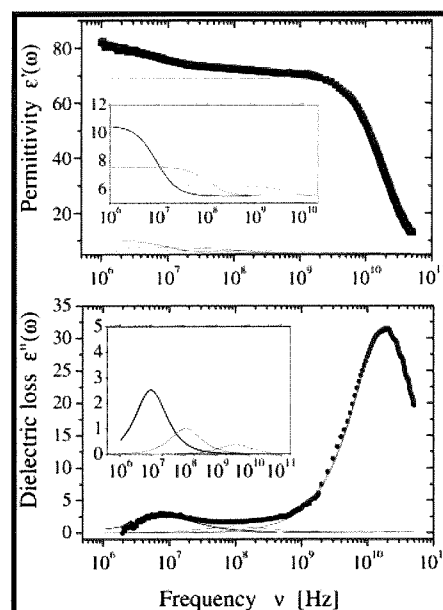


Figure 3. Dielectric spectra of lysozyme aqueous solution ($C = 110$ mg/mL) as a function of frequency at the temperature of 20 °C. Upper panel: the permittivity $\epsilon'(\omega)$ in the frequency range from 1 MHz to 50 GHz. The full lines represent the calculated values on the basis of eq 3. The inset shows in an enlarged scale the low-frequency tail of the spectrum and its deconvolution by three single Debye-type relaxation functions. Bottom panel: the dielectric loss in the same frequency range. The inset shows the deconvolution of the spectrum in its low-frequency tail.

3. RESULTS AND DISCUSSION

Dielectric spectra have been analyzed by means of the above stated relaxation functions (eqs 2 and 3) according to the protein concentration. Typical dielectric spectra (both the permittivity $\epsilon'(\omega)$ and the dielectric loss $\epsilon''(\omega)$), together with their spectral deconvolution, are shown in Figure 2 (for the low-concentration range, $C = 28$ mg/mL) and in Figure 3 (for the high concentration range, $C = 110$ mg/mL).

The loss spectra shown in the bottom panels of Figures 2 and 3 indicate that, without imposing any relaxation model, two relaxation processes emerge centered at about 10 MHz (β -relaxation) and 10 GHz (γ -relaxation). Simultaneously, a negative excess polarization appears for the bulk water relaxation without exhibiting a significant shift of the loss peak frequency. In the whole concentration range investigated, in addition to the β - and γ -dispersions, we observed an intermediate δ -dispersion which is characterized to be monomodal in the low-concentration range (up to about 50 mg/mL) and bimodal in the high-concentration range (from about 50 to 120 mg/mL).

A satisfactory estimation of the parameters $\Delta\epsilon$, and $\nu = 1/(2\pi\tau)$ for each relaxation regions considered has been obtained using a nonlinear least-squares fitting procedure based on the Levenberg–Marquardt algorithm⁷ for complex functions. The method allows simultaneous fits of the permittivity $\epsilon'(\omega)$ and the dielectric loss $\epsilon''(\omega)$ with the same set of free parameters by minimizing the deviation D ,

$$D = \frac{1}{2(n-m)} \left[\left(\sum_{i=1}^n (\epsilon'(\omega_i) - \epsilon'_{\text{calcd}}(\omega_i))^2 + \sum_{i=1}^n (\epsilon''(\omega_i) - \epsilon''_{\text{calcd}}(\omega_i))^2 \right)^{1/2} \right] \quad (6)$$

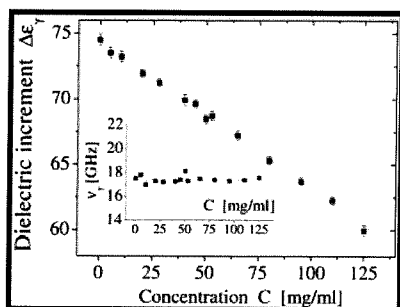


Figure 4. Dielectric increment $\Delta\epsilon_\gamma$ of the γ -dispersion of lysozyme aqueous solution as a function of the protein concentration C . The inset shows the relaxation frequency ν_γ as a function of the lysozyme concentration C .

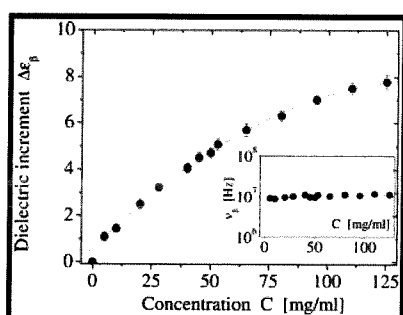


Figure 5. Dielectric increment $\Delta\epsilon_\beta$ of the β -dispersion of lysozyme aqueous solution as a function of the protein concentration C . The inset shows the relaxation frequency ν_β as a function of the lysozyme concentration C .

where n is the number of data points in the dielectric spectrum, m is the number of free fitting parameters and $\epsilon_{\text{calcd}}'(\omega_i)$ and $\epsilon_{\text{calcd}}''(\omega_i)$ are the real and imaginary parts of the fitting function values at frequency ω_i , respectively. Details of this procedure are fully discussed elsewhere.^{19,16} Briefly, we have made a preliminary simultaneous fit of the permittivity $\epsilon'(\omega)$ and the total dielectric loss $\epsilon_{\text{tot}}''(\omega) = \epsilon''(\omega) + \sigma_0/(i\omega\epsilon_0)$ with 7 (eq 2) or 8 (eq 3) free parameters and with the only constraint that all the parameters should be positive. The value of σ_0 thus obtained is then subtracted from the measured conductivity $\sigma(\omega)$, the dielectric loss is evaluated and a new set of parameters from the simultaneous fit of both the permittivity $\epsilon'(\omega)$ and dielectric loss $\epsilon''(\omega)$ are now obtained. This procedure is iterated until a reasonable minimization is reached and the parameters $\Delta\epsilon$, ν , and σ_0 converge to stable values. A further check of the goodness of the fit we performed can be found in the values we have obtained for the parameter σ_0 which, within the derived uncertainties, agree with the value measured directly in the low-frequency limit.

The accuracy in the evaluation of the dielectric parameters, i.e., the dielectric increment $\Delta\epsilon$ and the relaxation frequency ν , depends on the magnitude of the dielectric relaxation (i.e., mainly on the protein concentration) and on the algorithm employed in the fitting procedure. An accurate analysis based on different initialization conditions in the Levenberg–Marquardt method results in uncertainties of the order of 1% in the dielectric increment $\Delta\epsilon$ and 2–3% in the relaxation frequency ν , in the more unfavorable situations.

The dielectric parameters, i.e., the dielectric increment $\Delta\epsilon$ and the relaxation frequency ν associated with the different relaxation regions we have observed, deduced from the fitting of eqs 2 and 3

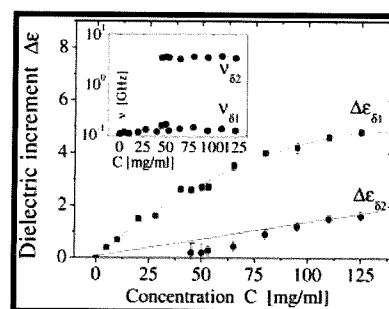


Figure 6. Dielectric increments $\Delta\epsilon$ associated with the two components $\Delta\epsilon_{\delta 1}$ and $\Delta\epsilon_{\delta 2}$ of the δ -dispersion of lysozyme aqueous solution as a function of the protein concentration C . Due to the small strength of the δ_2 -dispersion, values in the low concentration range are affected by large uncertainties and consequently we have assumed a linear dependence over the whole concentration interval. The inset shows the relaxation frequencies $\nu_{\delta 1}$ and $\nu_{\delta 2}$ as a function of the lysozyme concentration C for the two relaxation regions.

to the experimental spectra are shown in Figures 4 and 5, as far as the β - and γ -dispersion are concerned and in Figure 6 for the δ -dispersion.

In what follows, we will analyze in detail each relaxation region and we will discuss the meaning of the parameters characterizing the protein solution we have obtained.

3.1. Parameters Extracted from the β -Dispersion. The knowledge of the dielectric parameters of the β -dispersion, the dielectric increment $\Delta\epsilon_\beta$ and the relaxation time $\tau_\beta = 1/(2\pi\nu_\beta)$, allows us to evaluate the hydrodynamic radius R of the protein and its electrical dipole moment μ . In an orientational process controlled by the hydrodynamic friction with the solvent, the relaxation time of a globular (spherical) protein of hydrodynamic radius R in a medium of viscosity η is given by the Debye expression,²⁰

$$\tau_\beta = \frac{4\pi R^3 \eta}{K_B T} \quad (7)$$

with $K_B T$ the thermal energy. Assuming for the aqueous medium viscosity a value of $\eta = 0.90 \cdot 10^{-3}$ Pa s (at 298 K), eq 7 yields $R = 17.9$ Å, largely independent of the protein concentration. This value is in good agreement with previous results.²¹ The independence of R of the protein concentration, contrarily to what happens in the hydrodynamic radius estimated by means of dynamic light scattering measurements, is attributed to the minor influence of protein–protein interactions on rotational dynamics compared to the diffusional dynamics,²² where electrostatic interactions due to the net charge of the protein dominate.²³

The form factor derived from small-angle neutron scattering experiments on lysozyme solutions at different concentrations²⁴ furnishes for the two semiaxes of the prolate ellipsoid values of $a = 21.9$ Å and $b = 13.5$ Å, respectively. The value of the hydrodynamic radius R we have estimated from dielectric measurements compares, in the limit of the spherical approximation, with these data reasonably well.

The effective dipole moment of the lysozyme in solution, within the Onsager–Oncley model,⁷ is related to the dielectric increment $\Delta\epsilon_\beta$ by the relation,

$$\mu_{\text{eff}}^2 = \frac{2\epsilon_0 K_B T \Delta\epsilon_\beta}{N_A C} \quad (8)$$

where N_A is the Avogadro number and C the protein concentration. The dipole moment μ_{eff} of the protein depends on its

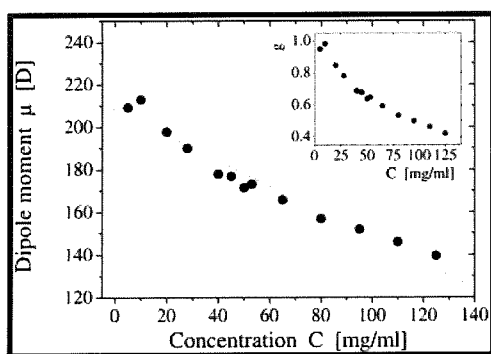


Figure 7. The effective dipole moment μ of lysozyme in aqueous solution at the temperature of 25 °C, as a function of the concentration C , derived from the dielectric strength of the β -dispersion. The inset shows the protein–protein Kirkwood factor.

environment, since a reaction field exists even in the absence of an external field, leading to an increase of the dipole moment as compared with that of the isolated molecule.²⁵ Equation 8 represents a generalization of the Debye theory, taking into account internal field effects. There are, however, other slightly different expressions based on slightly different assumptions in the dielectric model adopted. For example, a widely used expression considers the dielectric increment $\Delta\epsilon_\beta$ corrected with parameters of the whole dispersion according to the relationship,

$$\mu_{\text{eff}}^2 = \frac{9\epsilon_0 K_B T (2\epsilon_s + \epsilon_\infty) \Delta\epsilon_\beta}{\epsilon_s (\epsilon_\infty + 2) N_A C} \quad (9)$$

where ϵ_s and ϵ_∞ are the low-frequency and the high-frequency limit of the permittivity ϵ' associated to the β -dispersion. However, these expressions do not differ too much from one another.²⁶

From eq 8 and the values of the dielectric increment $\Delta\epsilon_\beta$ already obtained, the values of the apparent dipole moment of the lysozyme molecule in solution can be properly evaluated. The results are reported in Figure 7. As can be seen, eq 8 evidences an *apparent* decrease of the dipole moment μ with the protein concentration. The apparent dipole moment is related to the one of the isolated protein μ_0 by the Kirkwood relationship $\mu_{\text{app}}^2 = g\mu_0^2$ where g is the protein–protein orientational correlation factor. The effective dipole moment μ_0 can be determined by extrapolation of the apparent dipole moment to zero protein concentration. The linear regression of the data yields $\mu_0 = 208 \pm 2.8$ D, with a linear correlation of $R = -0.9741$. The dependence of the Kirkwood parameter g on the lysozyme concentration is given in the inset of Figure 7. This parameter decreases with increasing protein concentration. Oleinikova et al.⁹ attributed this peculiar feature to the strong antiparallel dipolar correlation between protein molecules, favored by their relatively high dipole moments. According to South and Grant,²⁷ the major contribution to the dipole moment arises from the rotational relaxations of the protein molecule as well as from effects associated with the migration and redistribution of proton at the protein surface, as described by Kirkwood and Shumaker.²⁸ A further contribution to dipole–dipole interactions arises from the tendency of lysozyme to cluster at concentrations lower than 20%, as evidenced from small-angle neutron scattering measurements.^{24,29} The results obtained from the fit of neutron scattered intensity clearly evidence that the protein interparticle distance is systematically smaller than the mean distance expected from protein concentration ($\sim C^{-1/3}$). The formation of small

equilibrium clusters in lysozyme solutions ($C = 40$ mg/mL, pH = 7.8) due to a combination of long-range repulsion and short-range attraction interactions has been also confirmed by Stradner et al.³⁰ on the basis of small-angle X-ray (SAXS) and neutron (SANS) measurements.

3.2. The Hydration Water. The δ -dispersion manifests as due to the orientational relaxation of dipoles of water in the hydration shell. Its deconvolution into two well-separated components induces us to attribute the δ_1 -component (roughly at 100 MHz) to tightly bound water and the δ_2 -component (roughly at 4–5 GHz) to loosely bound water. The hydration shell is heterogeneous at a molecular level and further distinction on the structure of the hydration water could be attempted on the basis of dielectric measurements.

The hydration number, reflecting the total number of water molecules affected by the protein, can be deduced either from the strength of the δ -dispersion or from the strength of the γ -dispersion. In this latter case, the amplitude of the γ -dispersion decreases with the increase of the protein concentration and this decrease is more marked than the one simply due to the presence of the protein in solution, suggesting that further water molecules do not contribute to the γ -dispersion, making its strength $\Delta\epsilon_\gamma$ lower than the one simply attributable to the presence of the protein.^{8,31} Oleinikova et al.⁹ suggested that a very simple method consists in the comparison of the dielectric increment $\Delta\epsilon_\delta$ to the one $\Delta\epsilon_\gamma$ of the γ -dispersion, this ratio being proportional to the ratio of water content in the shell around the protein and the water in the unaffected volume. As a matter of fact, as pointed out by Mashimo et al.,³² the dielectric strength is a measure of the water content multiplied by square of its dipole moment. If the polarity is not much changed by the protein, then the ratio $\Delta\epsilon_\delta/\Delta\epsilon_\gamma$ will be equal to the ratio of bound to free water.

Another option is to estimate the hydration water from the strength of the δ -dispersion, on the basis of the interfacial polarization model of heterogeneous systems. Because of the bimodal structure of the δ -dispersion, at least in the high concentration range, this approach offers the possibility to differentiate the behavior of tightly bound and loosely bound water.

In the light of the heterogeneous system dielectric model, the protein solution can be considered as a collection of spherical particles of complex dielectric constant $\epsilon_p^*(\omega) = \epsilon_p(\omega) + \sigma_p/(i\epsilon_0\omega)$, covered by a concentric shell of complex dielectric constant $\epsilon_h^*(\omega) = \epsilon_h(\omega) + \sigma_h/(i\epsilon_0\omega)$ and uniformly distributed in a continuous medium of complex dielectric constant $\epsilon_m^*(\omega) = \epsilon_m(\omega) + \sigma_m/(i\epsilon_0\omega)$. The complex dielectric constant $\epsilon^*(\omega)$ of the whole system is given by the following:

$$\epsilon^*(\omega) = \epsilon_m(\omega) \frac{2(1 - \Phi)\epsilon_m^*(\omega) + (1 + 2\Phi)\epsilon_{\text{eq}}^*(\omega)}{(2 + \Phi)\epsilon_m^*(\omega) + (1 - \Phi)\epsilon_{\text{eq}}^*(\omega)} \quad (10)$$

where the equivalent complex dielectric constant $\epsilon_{\text{eq}}^*(\omega)$ of the shelled particle is given by the following:

$$\epsilon_{\text{eq}}^*(\omega) = \epsilon_h^*(\omega) \frac{2(1 - \Phi_p)\epsilon_h^*(\omega) + (1 + 2\Phi_p)\epsilon_p^*(\omega)}{(2 + \Phi_p)\epsilon_h^*(\omega) + (1 - \Phi_p)\epsilon_p^*(\omega)} \quad (11)$$

Here, $\Phi = (N_p/V)(4\pi/3)(R_p + d)^3$ is the volume fraction of the shelled particles (proteins covered with the hydration shell) and $\Phi_p = R_p^3/(R_p + d)^3$ the volume fraction of the bare protein with respect to the volume which encompasses the hydration water. N_p/V is the numerical concentration of the proteins of radius R_p and d is the thickness of the hydration shell. The

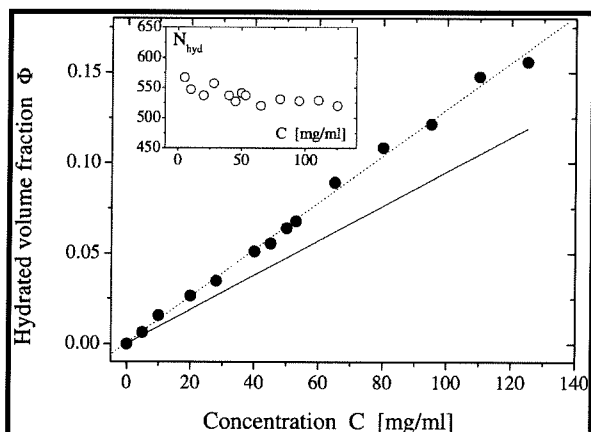


Figure 8. The hydrated volume fraction Φ of protein solution as a function of the concentration C , obtained from the analysis of the δ -dispersion, following the method of Yokoyama et al.⁸ The continuous line represents the values of volume fraction of bare protein solution. The inset shows the hydration number obtained from the hydrated volume fraction Φ .

volume fraction Φ_p can be expressed through the relationship $\Phi_p = \Phi_0/\Phi$, where $\Phi_0 = (N_p/V)(4\pi/3)R_p^3 \equiv C\nu_0$ is the volume fraction of the bare protein, with C the concentration of the protein in g/mL and ν_0 its partial specific volume expressed in mL/g. Within this approach, we do not differentiate the dielectric behavior of different kinds of hydration water and we attribute to the hydration shell, as a whole, a unique value ϵ_h of the dielectric constant.

This approach, aimed to obtain the volume Φ from the experimental data in the region where the δ -dispersion falls, was adopted, in particular, by Wei et al.³³ Using their method, the amount of hydration water in the solution and then the hydration number (i.e., the number of hydrated water molecules per each protein molecule) can be easily obtained from the difference between the total mass of water (M_W/V) and the one of the free water (M_{Wf}/V) per volume V . This difference is given by the following:

$$\frac{M_W}{V} - \frac{M_{Wf}}{V} = (\rho - C) - \rho_0(1 - \Phi) \quad (12)$$

where ρ and ρ_0 are the densities of the solution and of the aqueous phase ($\rho_0 = 0.9971$ g/mL at 25 °C), C is the protein concentration expressed in g/mL. Consequently, the hydration number is given by the following:

$$N_{\text{hyd}} = \left(\frac{M_W}{V} - \frac{M_{Wf}}{V} \right) \frac{M_{wp}}{M_{w0}C} \quad (13)$$

where M_{w0} and M_{wp} are the molecular weight of water and protein, respectively. In this approach, as pointed out by Wei et al.,³³ the evaluation of N_{hyd} is based only on the measurement of the low-frequency limit of the permittivity $\epsilon'(\omega)$ and on the density ρ of the solution. Other quantities, such as the dry volume of the protein, are not necessary.

In eqs 10 and 11, the following approximations hold,^{26,34} $\epsilon_h^*(\omega) \equiv \epsilon_h = 5.6$ and $\epsilon_p^*(\omega) \equiv \epsilon_p = 2.5$. The procedure suggested by Yokoyama et al.⁸ allows us to evaluate the fractional volume Φ , and hence the hydration number, considering the dielectric increment $\Delta\epsilon_\delta = \Delta\epsilon_{\delta_1} + \Delta\epsilon_{\delta_2}$ derived from the solution of eqs 10 and 11. The results are shown in Figure 8,

where we report the fractional volume Φ of the hydrated protein solution (compared with the fractional volume Φ_0 of the bare proteins in solution) and the hydration number N_{hyd} calculated according to eq 13. We obtain a number of water molecules per lysozyme molecule of about $N_{\text{hyd}} \approx 525$. This value is, to a first approximation, constant over the whole concentration range investigated. The slight increase of N_{hyd} at the lower concentrations (inset of Figure 8) is attributable to the large uncertainties in the evaluation of $\Delta\epsilon_\delta$ where the dielectric strength progressively reduces as the protein concentration approaches zero. Considering that lysozyme has 79 polar residues, encompassing weakly polar, meanly polar and ionizable residues, we estimate an average hydration number per amino-acid residue of about 6.6. As far as the volume fraction Φ is concerned, its value is in very good agreement with the ones derived by Yokoyama et al.⁸ for lysozyme solution in low concentration regime (up to 35 mg/mL), whereas the value of N_{hyd} we obtain is a little bit higher. However, the analysis carried out by Yokoyama et al.⁸ extends over a narrower frequency range (from 0.2 to 20 GHz) than the one investigated here and consequently the relaxation function employed models basically the δ -dispersion only (or probably the δ_2 -dispersion only) and partially the γ -dispersion. On the basis of the decrement of the permittivity measured at a single frequency (5.13 GHz), Rejoul-Michel et al.³⁵ evaluated a hydration number of about 450 water molecules per lysozyme molecule, which corresponds to 1.25 layers of bound water. The value of N_{hyd} we have found represents the number of hydration water overall involved in the vicinity of the protein surface. Considering that the inner hydration shell engages about 346 water molecules per protein, corresponding to the fully monolayer coverage of the protein surface, as observed from small-angle neutron scattering,³⁶ our result indicates the presence of a further amount of hydration water. This water is just what the δ_2 -dispersion takes into account.

3.3. The δ_2 -Relaxation Region. In the present case, at the higher lysozyme concentrations, we have found that a further contribution, denoted as δ_2 -dispersion, manifests, indicating the presence of a fraction of hydration water that is loosely bound, with a relaxation frequency intermediate between the one of free water and strongly bound water. This contribution is too small to be experimentally evidenced in the lower concentration range, up to approximately 45–50 mg/mL, where the δ -dispersion appears to be monomodal.

The question now arises how to identify the amount of this contribution with respect to the total hydration water. In order to do this, it may be helpful to first derive the ratio between the dielectric increment $\Delta\epsilon_{\delta_2}$ of the δ -dispersion to the one ($\Delta\epsilon_{\delta_1} + \Delta\epsilon_{\delta_2}$) of the total δ -dispersion. This quantity is assumed to be a measure of the ratio between the loosely bound hydration water to the total hydration water and hence a measure of the number N_{hyd}^L of loosely bound water per protein molecule. Figure 9 shows the dependence of $\Delta\epsilon_{\delta_2}/(\Delta\epsilon_{\delta_1} + \Delta\epsilon_{\delta_2})$ and N_{hyd}^L as a function of the protein concentration C . It must be noted that the amplitude of the δ_2 -dispersion is rather small, particularly at the lower concentrations, with values of the dielectric increment $\Delta\epsilon_{\delta_2}$ smaller than one dielectric unit. This causes a large uncertainty in the evaluation of the hydration number N_{hyd}^L when the protein concentration is smaller than 45–50 mg/mL. In order to compensate for this difficulty, we have considered a linear dependence of $\Delta\epsilon_{\delta_2}$ on the concentration C over the whole concentration range investigated and we have estimated N_{hyd}^L on the basis of this linear dependence (see inset of Figure 9). However,

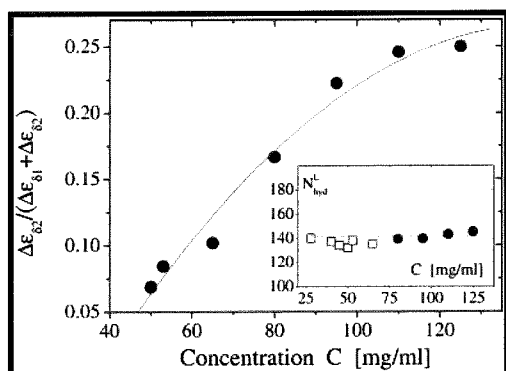


Figure 9. The ratio $\Delta\epsilon_{\delta 2}/(\Delta\epsilon_{\delta 1} + \Delta\epsilon_{\delta 2})$ as a function of the protein concentration C . This quantity represents the loosely bound to the total bound hydration water ratio. The inset shows the hydration number N_{hyd}^L per protein molecule as a function of the concentration C . Full circles: values calculated on the basis of the measured dielectric strength at higher protein concentration; open squares: values calculated on the basis of the assumed linear dependence of $\Delta\epsilon_{\delta 2}$ in the lower concentration interval.

when the protein concentration is large enough, N_{hyd}^L tends to a constant value of the order of $N_{\text{hyd}}^L = 150$.

Yokoyama et al.⁸ have evaluated the amount of the hydration water on the basis of a three-dimensional protein structure considering the accessible surface area of both polar and apolar atoms exposed on the protein molecules. They associate the number of tightly bound water molecules N_{hyd}^T to the water accessible to polar atoms (N, O) and the number of loosely bound water molecules N_{hyd}^L to water accessible to hydrophobic surface ($-\text{CH}_x$) of the protein. These values are $N_{\text{hyd}}^T = 150$ and $N_{\text{hyd}}^L = 180$, respectively. Our results reasonably agree with a picture that considers a tightly bound hydration shell with a thickness close to a layers of water followed by a further layer of more loosely bound water layer.

3.4. Bulk Water Relaxation. The dielectric properties of water at microwave frequencies have been reviewed by Kaatzte et al.^{37,38} on the basis of available literature data. These authors found that a simple Debye-type function is appropriate to describe the dielectric behavior, characterized, at a temperature of 20 °C, by a dielectric increment $\Delta\epsilon = (74.59 \pm 0.35)$ and by a relaxation time $\tau = (9.36 \pm 0.05)$ ps, obtained by a nonlinear regression analysis of the literature data. These values agree reasonably well to the ones we have measured on pure water and, moreover, to the ones obtained from extrapolation to zero protein concentration. In the presence of protein, as already indicated by the negative excess loss spectrum of the γ -relaxation, $\Delta\epsilon_\gamma$ always exhibits smaller values than expected from *analytical* water concentration. The definition of hydration water we have adopted includes all the water molecules that do not contribute to the free-water relaxation, at least, from a dielectric point of view.

Using the values of $\Delta\epsilon_\gamma$ as a function of the protein concentration C , we estimated the effective hydration number on the basis of the Cavel equation^{39–41} (for spherical molecules):

$$\frac{2\epsilon + 1}{\epsilon} \Delta\epsilon_w = \frac{N_a C_w}{K_B T \epsilon_0} \mu^2 \quad (14)$$

which connects the dielectric increment $\Delta\epsilon$ to the concentration C_w of the relaxation species through the static permittivity ϵ , the effective dipole moment $\mu = \mu_0/(1 - \alpha_w f_w)$ of water, with μ_0 its permanent dipole, α_w its polarizability and f_w the reaction field

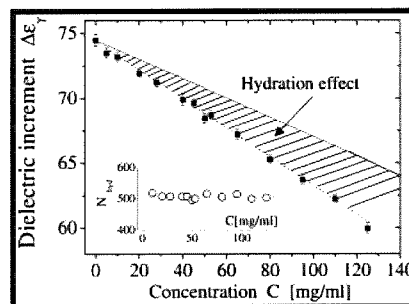


Figure 10. The dielectric increment $\Delta\epsilon_\gamma$ as a function of the protein concentration C derived from the analysis of the γ -dispersion. The continuous line represents the ideal bulk-water amplitude calculated (eq 15) from the analytical water concentration under the assumption that all water molecules in the solution contribute to the bulk water process with the same Kirkwood dipole–dipole orientational correlation factor of pure water. The inset shows the hydration number calculated on the basis of eq 16 as a function of the protein concentration C .

factor. $K_B T$ is, as usual, the thermal energy and N_A the Avogadro number. Equation 14, normalized to pure water, yields the apparent water concentration $C_w(C)$

$$C_w(C) = \frac{\Delta\epsilon_\gamma(C)}{\Delta\epsilon_\gamma(0)} \frac{\rho_0}{M_{w0}} \quad (15)$$

where we put $\Delta\epsilon_\gamma(0) = 74.5$ (at $T = 20$ °C). Equation 15 allows us to deduce the concentration of water molecules contributing to the bulk water relaxation and the effective hydration number:⁴²

$$N_{\text{hyd}} = \frac{C_w(0) - C_w(C)}{C} \quad (16)$$

as the number of water molecules per protein that cannot contribute to the bulk water relaxation process due to the hydration effect. Figure 10 shows the dielectric increment $\Delta\epsilon_\gamma$ derived from the analysis of the γ -dispersion on the basis of a Debye relaxation function compared to the dielectric increment calculated from eq 15, considering the *analytical* water concentration. The hydration effect results in a hydration number N_{hyd} of the order of about 500 water molecules per protein molecule, independent of the protein concentration. This value, derived from the total amount of water affected by the presence of the protein, is in reasonable good agreement with the one derived from the δ -dispersion.

Some final comments are in order. The bimodal character of the δ -relaxation of water near a biomolecule is rather universal, even if its explanation is still controversial. Further insights on the δ -processes, and on their consequent assignment, have been obtained from investigations on hydrated lysozyme powders (hydration of the order of $h = 0.35$, measured in g of water per g of dry protein), since in these conditions, protein tumbling (β -relaxation) is strongly slowed down and there is no bulk water (γ -relaxation) at these hydrations. This hydration level corresponds to the point at which the first hydration shell is completed and bulk water begins to accumulate.⁴³ Recently, Khodadadi et al.,⁴⁴ on the basis of combined neutron scattering and dielectric spectroscopy measurements, found, at temperatures higher than 250 K, two different contributions. The fastest of these is ascribed to water of protein hydration (with characteristics similar to those observed in aqueous protein solutions). A process with a similar relaxation time has been reported by Chen et al.⁴⁵ on the basis of a neutron scattering investigation on hydrated lysozyme ($h = 0.30$), where the independence of the relaxation time of the

scattering wave vector is a hint for the assignment of the process to the hydration water.

The assignment of the slowest relaxation process is a little bit more controversial. Although it is generally attributed to water of hydration tightly bound to the protein surface,^{46–48} one cannot exclude, in principle, that this process could result from a cross term in the relaxation of dipoles of hydration water and dipoles of the protein.^{9,11} These hypotheses are supported by simulations and NMR measurements that have evidenced that water molecules are moving on a time scale 2–3 times slower than bulk water.⁴⁹ Moreover, most of the hydration water exchange with the bulk on a time scale shorter than 50 ps.⁵⁰ A model that reconciles the different point of view has been proposed by Nandi and Bagchi,⁵¹ in terms of a two-state model, based on a dynamical equilibrium between the loosely bound and the tightly bound water molecules. The model shows that only the loosely bound water (termed *free water* by Nandi and Bagchi⁵¹) contributes to the relaxation process (fastest component), while the slow relaxation depends substantially on the strength of hydrogen bonds. However, since the dynamics of the bound water is coupled to the biomolecular rotation, in this model, the slowest component of the dispersion re-experiences the protein tumbling. In this context, the bimodality of the dielectric relaxation must be attributed to the reorientational response of the hydration water (both loosely and tightly bound water). This water in the immediate vicinity of the protein is appropriately termed *biological water*.

4. CONCLUSIONS

Dielectric spectroscopy is a valuable tool for studying the structure and the dynamics of protein solution. However, the resulting spectra, extending over a wide frequency range and presenting a multicomponent structure are not always easy to be interpreted. The deconvolution of the spectra into the single components, and the subsequent assignment to different polarization mechanisms at a molecular level, is generally a difficult task, where caution is obligatory. We have investigated the dielectric properties of lysozyme aqueous solution over an extended frequency range covering the interval from 1 MHz to 50 GHz. In this frequency window, basically three different relaxations occur, associate to a protein tumbling, characterized by a reorientation time of the order of 10–15 ns, to a relaxation of the hydration water, with times on the order of 0.05–5 ns, and, finally, to the orientational polarization of the water molecules, at times of the order of 8–10 ps. While the attribution of the two outer relaxation processes is well-defined, and consequently unambiguous, for the analysis of the spectra, the situation is a little bit more intricate, as far as the intermediate relaxation, associated to the hydration water, is concerned.

In this work, we analyze in detail the structure of this intermediate frequency range and, on the basis of a statistical analysis, we observed a monomodal and a bimodal relaxation spectrum, depending on the protein concentration. In the low-concentration regime (up to about 50 mg/mL), a single Debye-type relaxation function is able to account for the experimental data with enough degree of accuracy, so that more sophisticated analyses are neither substantiated nor required by the data. Contrarily, in the high concentration interval, we are forced to introduce a further Debye-type relaxation function, evidencing the bimodal nature of the dispersion. From the complete deconvolution of the spectra, we have evaluated the amount of the

water affected by the presence of the protein (hydration water) and characterized the hydration numbers as far as the two different species of hydration water (tightly bound and loosely bound hydration water) are concerned. In our opinion, the analysis suggested here forms an option consistent with the experimental data. There are two types of hydration water molecules in lysozyme solution, which are strongly and weakly associated with the protein molecule. Only the strongly associated water was distinguishable over the whole protein concentration range investigated, while the weakly associated water was observable, at least from dielectric methods as those employed here, only at higher protein concentrations. The total amount of hydration water has also been obtained from the loss spectrum of the free water (γ -dispersion), whose decrease is more marked than the one simply due to the presence of the protein in solution. The two approaches furnish results in rather good agreement and allow us to identify and characterize the hydration water in lysozyme aqueous solutions, at least from a dielectric point of view. However, it is important to emphasize that other definitions are possible, based on different experimental methods, such as IR and calorimetric measurements.⁵² Comprehensive dielectric data on the hydration property of more or less organized biostructures are still lacking and the appearance of a contribution to the hydration water depending on protein concentration deserves to be further investigated.

■ AUTHOR INFORMATION

Corresponding Author

*Fax: +39 06 4463158; E-mail: cesare.cametti@roma1.infn.it.

■ REFERENCES

- (1) Pal, S. K.; Peon, J.; Bagchi, B.; Zewail, A. H. *J. Phys. Chem. B* **2002**, *106*, 12376–12395.
- (2) Bull, H. B.; Breese, K. *Arch. Biochim. Biophys* **1968**, *128*, 488–498.
- (3) Ritland, H. N.; Kaesberg, P.; Beeman, N. W. *J. Chem. Phys.* **1950**, *18*, 1237–1242.
- (4) Svergun, D. I.; Richard, S.; Kock, M. H. J.; Sayers, Z.; Kuprin, S. *Proc. Natl. Acad. Sci. U.S.A.* **1998**, *95*, 2267–2272.
- (5) Kubinek, M. G.; Wemmer, D. E. *Curr. Opin. Struct. Biol.* **1992**, *2*, 828–831.
- (6) Subramanian, S.; Fisher, H. F. *Biopolymers* **1972**, *11*, 1305–1310.
- (7) Grant, E.; Sheppard, R.; South, G. *Dielectric Behaviour of Biological Molecules in Solution*; Clarendon Press: Oxford, UK, 1978.
- (8) Yokoyama, K.; Kamey, T.; Miami, H.; Suzuki, M. *J. Phys. Chem. B* **2001**, *105*, 12622–12627.
- (9) Oleinikova, A.; Sasisanker, P.; Weingartner, H. *J. Chem. Phys. B* **2004**, *108*, 8467–8474.
- (10) Nandi, N.; Bagchi, B. *J. Phys. Chem. B* **1997**, *101*, 10954–10961.
- (11) Nandi, N.; Bhattacharyya, K.; Bagchi, B. *Chem. Rev.* **2000**, *100*, 2013–2045.
- (12) Desinov, V. P.; Halle, B. *Acta Physicochim. URSS* **1996**, *103*, 227–243.
- (13) Pal, S. K.; Peon, J.; Zewail, A. H. *Proc. Natl. Acad. Sci. U.S.A.* **2002**, *99*, 1763–1768.
- (14) Poon, W. C. K.; Egelhaaf, S. U.; Beales, P. A.; Salonen, A.; Sawyer, L. *J. Phys.: Condens. Matter* **2000**, *12*, L569–L572.
- (15) Bordini, F.; Cametti, C.; Colby, R. H. *J. Phys.: Condens. Matter* **2004**, *R1423*–R1463.
- (16) Bordini, F.; Colby, R. H.; Cametti, C.; De Lorenzo, L.; Gili, T. *J. Phys. Chem. B* **2002**, *106*, 6887–6893.
- (17) Bao, J. Z.; Davis, C. C.; Swicord, M. L. *Biophys. J.* **1994**, *66*, 2173–2180.

- (18) Kremer, F.; Schönhal, A. *Broadband Dielectric Spectroscopy*; Springer: Berlin, 2003.
- (19) Bordi, F.; Cametti, C.; Gili, T. *Bioelectrochemistry* **2001**, *54*, 53–61.
- (20) Takashima, S. *Electrical Properties of Biopolymers and Membranes*; Adam Hilger: Bristol, 1989.
- (21) Bonincontro, A.; Cinelli, S.; Onori, G.; Stracato, A. *Biophys. J.* **2004**, *86*, 1118–1123.
- (22) Bonincontro, A.; Calandrini, V.; Onori, G. *Colloids Surf.* **2001**, *21*, 311–316.
- (23) Chirico, C.; Beretta, S.; Baldini, G. *J. Chem. Phys.* **1999**, *110*, 2297–2304.
- (24) Giordano, R.; Grasso, A.; Teixeira, J.; Wanderling, F.; Wanderling, U. *Phys. Rev. A* **1991**, *43*, 6894–6899.
- (25) Takashima, S. In *Physical Principles and Techniques of Protein Chemistry*; Leach, S. J., Ed.; Academic Press: New York, 1969; Chapter Dielectric Properties of Proteins. I. Dielectric Relaxation.
- (26) Pethig, R. *Annu. Rev. Phys. Chem.* **1992**, *43*, 177–205.
- (27) South, G. P.; Grant, E. H. *Proc. R. Soc. London* **1972**, *328 Ser. A*, 371–387.
- (28) Kirkwood, J. G.; Shumaker, J. B. *Proc. Natl. Acad. Sci. U.S.A.* **1952**, *38*, 855–858.
- (29) Giordano, R.; Salvato, G.; J.; Wanderling, F.; Wanderling, U. *Phys. Rev. A* **1990**, *41*, 689–696.
- (30) Stradner, A.; Sedgwick, H.; Cardinaux, F.; Poon, W. C. K.; Egelhaaf, S. U.; Schurteberger, P. *Nature* **2004**, *432*, 492–495.
- (31) Del Rosario, E. J.; Hammes, G. G. *Biochemistry* **1969**, *8*, 1884–1889.
- (32) Mashimo, S.; Kuwabara, S.; Yagihara, S.; Higasi, K. *J. Phys. Chem.* **1987**, *91*, 6337–6338.
- (33) Wei, Y. Z.; Kumbarkhane, A. C.; Sadeghi, M.; Sage, J. T.; Tian, W. D.; Champion, P. M.; Sridhar, S.; McDonald, M. J. *J. Phys. Chem.* **1994**, *98*, 6644–6651.
- (34) Pethig, R. *Dielectric and Electronic Properties of Biological Materials*; John Wiley: New York, 1979.
- (35) Rejou-Michel, A.; Henry, F.; de Villardi, M.; Delmotte, M. *Phys. Med. Biol.* **1985**, *30*, 831–837.
- (36) Crupi, V.; Majolino, D.; Migliardo, P.; Wanderling, U. *J. Mol. Struct.* **1999**, *180–181*, 141–145.
- (37) Kaatze, U. *J. Chem. Eng. Data* **1989**, *34*, 371–385.
- (38) Kaatze, U.; Uhlendorf Z. *Phys. Chemie* **1981**, *126*, 151–165.
- (39) Barthel, J.; Hetzenauer, H.; Buchner, R. *Ber. Bunsen-Ges. Phys. Chem.* **1992**, *96*, 1424–1432.
- (40) Sato, T.; Sakai, H.; Sou, K.; Buchner, R.; Tsuchida, E. *J. Phys. Chem. B* **2007**, *111*, 1393–1401.
- (41) Buchner, R. In *Novel Approach to the Structure and Dynamics of Liquids: Experiments, Theories and Simulations*; Samios, J., Durov, V. A., Eds.; NATO Science series III, Vol 133: The Netherland, 2004; Chapter Dielectric Spectroscopy of Solutions
- (42) Schrödle, S.; Hefter, G.; Kunz, W.; Buchner, R. *Langmuir* **2006**, *22*, 924–932.
- (43) Rupley, J. A.; Careri, G. *Adv. Protein Chem.* **1991**, *41*, 37–172.
- (44) Khodadadi, S.; Rawlus, S.; Sokolov, A. P. *J. Phys. Chem B* **2008**, *112*, 14237–14280.
- (45) Chen, S.-H.; Liu, L.; Fratini, E.; Baglioni, P.; Faraone, A.; Mamontov, E. *PANS* **2006**, *103*, 9012–9016.
- (46) Bone, S.; Pethig, R. *J. Mol. Biol.* **1982**, *157*, 571–575.
- (47) Bone, S.; Pethig, R. *J. Mol. Biol.* **1985**, *181*, 323–326.
- (48) Harvey, S. C.; Hoeskstra J. *Phys. Chem.* **1972**, *76*, 2987–2994.
- (49) Modig, K.; Liepinsh, E.; Otting, G.; Halle, B. *J. Am. Chem. Soc.* **2004**, *126*, 102–114.
- (50) Oleinikova, A.; Smolin, N.; Brovchenko, I. *Biophys. J.* **2007**, *93*, 2986–3000.
- (51) Nandi, N.; Bagchi, B. *J. Phys. Chem. B* **1997**, *101*, 10954–10961.
- (52) Doster, W.; Bachleitner, A.; Dunau, R.; Hiebl, M.; Luscher, E. *Biophys. J.* **1986**, *50*, 213–219.